DOI 10.5862/JEST.249.13
УДК 621.73.011

V.S. Mamutov, A.V. Mamutov, S.N. Kunkin, X.S. Arsentyeva

METHOD OF OBTAINING FLD FOR USE IN SIMULATION OF METAL FORMING BY MOVABLE MEDIA

В.С. Мамутов, А.В. Мамутов, С.Н. Кункин, К.С. Арсентьева

ДИАГРАММЫ ПРЕДЕЛЬНЫХ ДЕФОРМАЦИЙ ТОНКОЛИСТОВОГО МЕТАЛЛА ПРИ ФОРМОВКЕ ПОДВИЖНЫМИ СРЕДАМИ

A combined numerical and experimental technique to obtain a Forming Limit Diagram of thin sheet metal for metal forming by movable media was developed. The technique is based on deforming sheet samples until failure by pressure of polyurethane into a variety of the elliptical dies. The required strain state is defined by the proportion of elliptical die window. Through-thickness strain of the sample near to a zone of failure or necking was measured, and major in-plane strains were obtained by finite-element simulation based on the known metal properties. The simplicity of measurements and the absence of a grid on the surface of the sample are the advantages of the suggested technique. Points of the Forming Limit Diagram for the specific thin sheet stainless steel where obtained.

METAL FORMING BY MOVABLE MEDIA; FORMING LIMIT DIAGRAM; COMBINED NUMERICAL-EXPERIMENTAL TECHNIQUE; DESTRUCTION OF SAMPLES BY PRESSURE OF POLYURETHANE; MEASUREMENT OF THICKNESS OF THE SAMPLE; FINITE-ELEMENT CALCULATION OF RELATIONSHIPS BETWEEN THE MAJOR STR.

Разработана расчетно-экспериментальная методика получения диаграммы предельных деформаций тонколистового металла для процессов формовки подвижными средами. Суть методики заключается в разрушении образцов давлением полиуретана при вариации размеров эллиптических матриц для создания требуемого деформированного состояния. В экспериментах и расчетах использованы матрица с круглым отверстием диаметром 100 мм и матрицы с овальными отверстиями с размерами 38х100 мм и 50х100 мм. Измеряется толщина образца вблизи зоны разрушения или шейкообразования и вычисляется деформация по толщине. Соотношения между главными деформациями определяются конечно-элементным расчетом на основе известной кривой деформационного упрочнения материала. Простота измерений, отсутствие сетки на поверхности образца являются достоинствами предлагаемой методики. Получены точки диаграммы предельных деформаций тонколистовой стали 12Х18Н10Т.

ЛИСТОВАЯ ФОРМОВКА ПОДВИЖНЫМИ СРЕДАМИ; ДИАГРАММА ПРЕДЕЛЬНЫХ ДЕФОРМАЦИЙ; РАСЧЕТНО-ЭКСПЕРИМЕНТАЛЬНАЯ МЕТОДИКА; РАЗРУШЕНИЕ ОБРАЗЦОВ ПОЛИУРЕТАНОМ; ИЗМЕРЕНИЕ ТОЛЩИННОЙ ДЕФОРМАЦИИ; КОНЕЧНО-ЭЛЕМЕНТНЫЙ РАСЧЕТ СООТНОШЕНИЯ ДЕФОРМАЦИЙ.

Introduction

The modern level of computers and finite-element (FE) complexes and their availability for simulation of sheet metal stamping enable numerical simulation and prediction of the stress-strain parameters of stamped blank with high precision. When using a general purpose FE code such as LS-DYNA®, it is possible to obtain the detailed distribution of all the components of deformation tensor at every moment during the deformation process [1]. In turn, it makes possible to achieve one of the important goals of the stamping process design – predicting the moment of the blank fracture using Forming Limit Diagrams (FLD) [2].

The processes of forming using elastomers (for instance polyurethane) have some differences from those where liquids are used as a pressure transmitting media. Both liquid and elastomer accumulate some

excessive energy during forming due to the uniform compression, but, unlike liquid, elastomers cannot leak through small openings, and pressure inside the media drops slower after plastic instability starts. In the work [3] experiments with piezoelectric sensors of pulse pressure were conducted performing calibration by a "pressure leap" technique using polyurethane. The experiments have shown that there is a time gap of 10–100 μs (depending on fractured material) from the beginning of plastic instability up to the fracture occurs, after that the pressure starts dropping rapidly. In the conditions of the pulse stamping, this resource of plasticity can be used for instance when a formed blank is stopped by a rigid die or by precise dosage of the pulse energy [4].

At loading with using the polyurethane until the moment of instability the blank is accelerated by accumulated energy to the high velocity, and the strain rate at the fracture zone can reach $de/dt = (1–5)\cdot 10^3\ s^{-1}$ [5]. Many of the works on obtaining and using FLD's, for instance [6], note that FLD at higher strain rates significantly differs from that obtained in quasistatic conditions. When simulating phenomena and processes with high strain rates such as Electro-Hydraulic Forming (EHF), Electro-Magnetic Forming (EMF), crash tests, etc., it is vital to provide FLD corresponded in terms of strain rates to the process that is simulated. The purpose of this work is the developing of a method of obtaining FLD of thin sheet metals for the processes of pulse stamping with elastomers.

Selection and rationale of the method of obtaining FLD

Stuart P. Keeler first suggested the empirical criteria of blank fracture based on measuring two planar principal strains at the moment before fracture starts [7]. Keeler obtained the FLDs for some carbon steels for the area where both principal strains are positive (i.e. the right part of diagram). The moment of fracture beginning was defined as the moment when plastic instability starts or, in other words, the moment when necking becomes visible. Later, Gorton M. Goodwin obtained similar data for the case when one of the principal strains is negative (i.e. the left part of the diagram) [8]. At the present time, the two variants of FLD are distinguished: when deformations are measured at the moment before necking and when the deformations are measured after the fracture occurred [2].

There are many ways to obtain FLD experimentally. All of them essentially are the destruction of the blank sample at predictable or measurable deformation conditions. The most popular are the Nakazima Test (by K. Nakazima [9]), Marciniak Test (by Z. Marciniak [10]), and also known from the beginning of the 20th century the Hydraulic Bulge Test when a clamped blank hydrostatically formed by liquid. The tests of Nakazima and Marciniak differ from each other mostly in shape of the punch – cylindrical with hemi-spherical end and cylindrical with flat end with rounded edges respectively. It is often called by combined name Nakazima-Marciniak test (fig. 1,*a*, *b*).

The essence of the Nakazima-Marciniak test is that the clamped blank sample of different shape is formed until the fracture using a punch. To reduce the effect from the friction between the punch and the blank in the Nakazima test, lubrication or a layer of antifriction material can be used. In the Marciniak test, a companion layer with a hole in the center or a punch with a center cut can be used which prevent the blank from touching the punch at the center.

The deformation state (the proportion between two principal planar strains ε_1 and ε_2) is defined by the shape and the size of the side cuts in the sample. The side cuts can be of different shape, but the most often used shape is circular cuts. A sample without cuts provides biaxial state of deformation at the center, which is: $\varepsilon_1 = \varepsilon_2$. A sample with maximum cuts gives an FLD point which approximately corresponds to the uniaxial tension, i.e. $\varepsilon_1 = -2\varepsilon_2$.

The actual principal strains are measured using a mesh or some pattern on the surface of the sample. This approach has some disadvantages. It is necessary to determine the moment of starting plastic instability, because this is the moment of fracture by definition. It is difficult to register such a moment by visual observation, so many researchers measured deformations after the fracture, and in this case measured strains included the necking deformation. Using a mesh or a pattern on the surface needs not only an operation of measuring this mesh but also corrections to take into account the neutral layer offset. In the past, that was done manually using a microscope and was very labor intensive. Now it is more common to use digital cameras and digital image correlation software which requires expensive hardware and software.

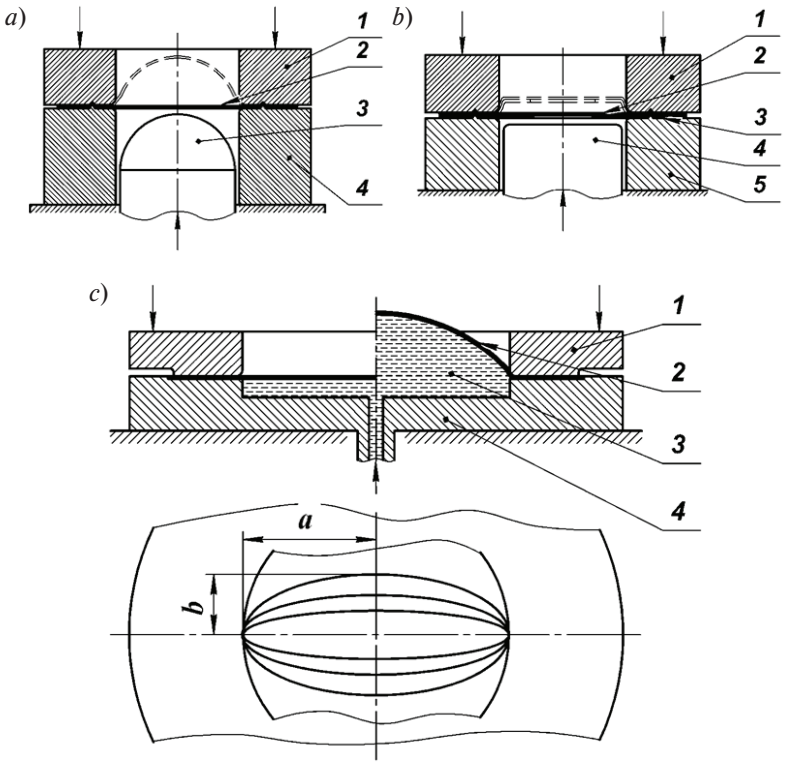

Fig. 1. Traditional methods of obtaining FLD: *a* – Nakazima Test (*1* – upper die, *2* – sample, *3* – spherical punch, *4* – lower die); *b* – Marciniak Test (*1* – upper die, *2* – sample, *3* – antifriction layer, *4* – cylindrical punch, *5* – lower die); *c* – Hydraulic Bulge Test (*1* – die, *2* – sample, *3* – liquid, *4* – chamber)

Furthermore, the mechanics of quasistatic deformation and fracture, which is typical conditions at Nakazima-Marciniak test, significantly differs from that at pulse stamping by movable media, such as EHF and EMF. From that perspective more appropriate is to use the Hydraulic Bulge Test (fig. 1, *b*). In this approach, forming of the sample 2 is performed by the hydrostatic pressure of liquid (usually oil) *3*, enclosed in chamber *4*. The die 1 has rounded edges to prevent fracture at the clamping contour. The proportion between principal strains is defined by the width *a* to height *b* dimensions of the elliptical die cavity. The equality $a = b$ creates uniaxial tensions ($\varepsilon_1 = \varepsilon_2$), and when $a >> b$, the second principal strain can be almost zero ($\varepsilon_2 \cong 0$).

That way it is possible to obtain the right part of FLD (with both principal strains positive). At the typical conditions of forming by movable media the right part of FLD is usually enough from practical perspective. Nevertheless, all the disadvantages of measuring strains are the same as in the Nakazima-Marciniak test. In this work, an experimental-numerical method of obtaining FLD similar to Hydraulic Bulge Test is suggested that allows measuring very close to the necking zone.

Combined experimental-numerical method of obtaining FLD

The prerequisite data for the method is the hardening curve in the form of the power law

$$\sigma_s = B \cdot \varepsilon_i^m,$$

where σ_s – true stress; ε_i – true strain; B and m – parameters of the power law approximation. The blank used in experiment was stainless steel 12X18H10T (approximate US equivalent is S32100) of thickness $h_0 = 0{,}55$ mm. The parameters of the power law were approximated as: $B = 1250$ MPa, $m = 0{,}287$. The experimental setup is shown in fig. 2,*a*.

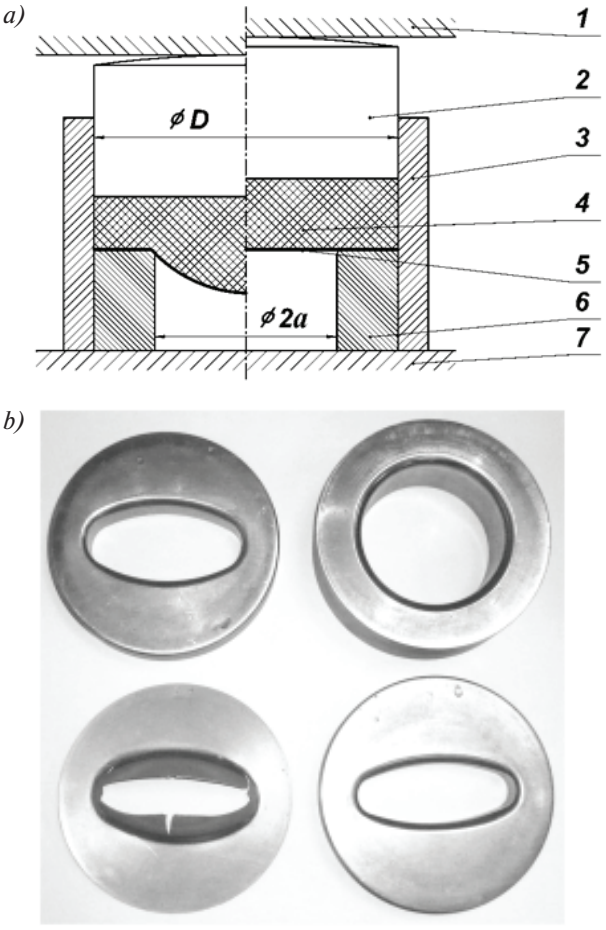

Fig. 2. Toolset for obtaining FLD: *a* – assembled toolset, cross-sectional view (*1*, *7* – die beds, *2* – piston, *3* – container-chamber, *4* – polyurethane, *5* – sample, 6 – die); *b* – die set: round-shaped, diameter – 100 mm; oval-shaped 38×100 mm, and 50×100 mm; the fractured sample corresponding the die 50×100 mm

Loading of the blank sample 5 is performed by the elastomer 4, enclosed in the container *3*, where pressure is created by moving the piston *2*. By pressure of the elastomer the sample is formed into the cavity of the die *6* until fracture. The hydraulic press of 100 tones was used.

The polyurethane with Shore hardness of 55–60 units was used as a pressure transmitting media. The friction coefficient is $\mu \leqslant 0{,}01$–$0{,}05$ for this type of polyurethane in the conditions of the given process [11]. Therefore it is not necessary to use antifriction layer between the blank and the elastomer. The polyurethane also serves as a binder that holds the flange of the sample *5* on the surface of the die *6*.

The inner radius of the round-shaped die as well as the major radius of the elliptic cavity of the oval-shaped die was $b = 50$ mm. The inside diameter of the container and corresponding outside diameter of the die was $D = 150$ mm. The sample diameter is 0,5 mm less than the container diameter. Although there is no special clamping of the flange, as it is usually done in the conventional test, such a proportion between the sample size and the die cavity size provides enough flange resistance and prevents flange from draw into the die thus ensuring that the strain (and the fracture) will happen in the center of the sample. The set of dies included round shaped die with radius 50 mm and two oval-shaped dies 50×19 mm, 50×25 mm. The edge fillet has the radius of 6 mm.

The chosen design of the toolset provided stable fracture conditions (fig. 2, *b*). After forming a sample up to the fracture, the thickness h of the sample was measured as close to the necking zone as possible using a dial indicator. About 5–10 measurements were taken for each sample with averaging the resulting value. Then the average true normal deformation is calculating as:

$$\varepsilon_h = \varepsilon_3 = \ln(h_0/h).$$

The round-shaped die provides uniaxial strain condition in the center of the sample ($\varepsilon_1 = \varepsilon_2$). For this point two principal strains are calculated as:

$$\varepsilon_1 = \varepsilon_2 = \varepsilon_3/2.$$

To obtain points of FLD other than for uniaxial strain it is needed to know the proportion between the major and the minor strain. That can be done using numerical simulation of the deformation process similar to that done in [12].

Simulation was performed with general purpose finite element complex LSDYNA 971. The material assumed as isotropic with the following parameters: Young modulus $E = 202$ GPa, Poisson coefficient $n = 0{,}31$; power law parameters: $B = 1250$ MPa, $m = 0{,}287$; density $\rho = 7800$ kg/m^3. The LSDYNA material card used was: *MAT_POWER_LAW_PLASTICITY*. The die was simulated as a rigid object. The friction assumed as Coulomb with friction coefficient changing from static $\mu = 0{,}2$ to dynamic $\mu = 0{,}15$. The pressure in the elastomer assumed linearly increasing from zero to maximum necessary to fracture the sample in 0,2 s. With given dimensions of the die and sample it provided nearly quasistatic forming conditions [12].

The results of the computer simulation are shown in fig. 3.

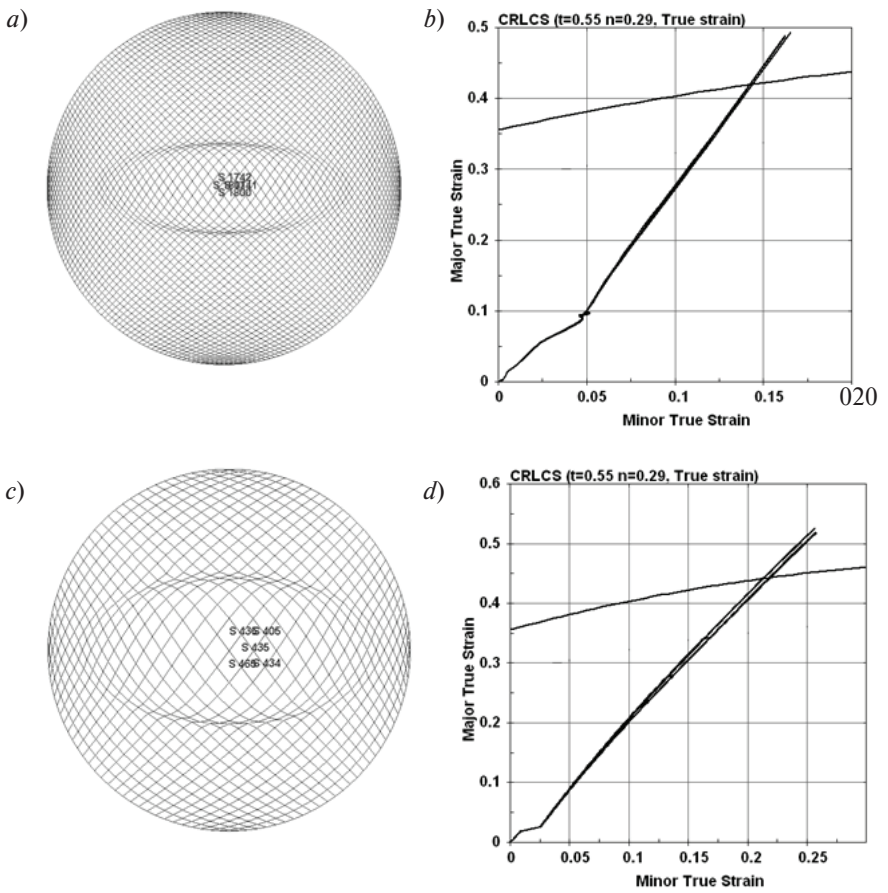

Fig. 3. Deformation paths for the marked points of the samples when forming in the oval-shaped dies 38×100 mm (*a*, *b*) and 50×100 mm (*c*, *d*) respectively

The diagrams on fig. 3,*b* and 3,*d* show paths of deformation at the center of the four samples. The same diagrams show the FLD obtained analytically from hardening data. The calculated deformation path defines the proportion between the principle strains $\alpha = \varepsilon_2/\varepsilon_1$. Together with the experimentally measured thinning (the third principal strain ε_3) it gives a point on FLD:

$$\varepsilon_1 = -\varepsilon_3/(1 + \alpha), \varepsilon_2 = \alpha\,\varepsilon_1.$$

The obtained FLD points are shown in tab. 1. The deviation of the measured thinning is 10–15%.

It can be noted that the obtained points are lower than that obtained from hardening data. It can be explained by the fact that the deformation in this experiment happens at high strain rate [5], which can cause such change in fracture limits [6]. The detailed distribution of FLD values in the range of $\varepsilon_2 > 0$ can be achieved by using dies with other proportion of the die cavity *a*/*b*.

Table

The components of the deformation tensor of the central point depending on the die

Shape of die cavity	*h*	$-\varepsilon_3$	$\alpha = \varepsilon_2/\varepsilon_1$	ε_2	ε_1
Round with radius 50 mm	0,25±0,02	0,79	1	0,395	0,395
Oval 50×100 mm	0,35±0,03	0,45	0,48	0,146	0,304
Oval 38×100 mm	0,38±0,03	0,37	0,35	0,096	0,274

Conclusion

The method of obtaining forming limit diagrams for thin sheet metal for using in simulation of pulse forming by movable media is developed. Because loading of the sample is performed by elastomer (polyurethane), the forming and fracture conditions in developed method are close to those in the said technologies such as electro-hydraulic and electromagnetic forming. The distribution of FLD values in the range of $\varepsilon_2 > 0$ can be obtained by using dies with different proportion of the elliptical die cavity. The range of FLD $\varepsilon_2 > 0$ is usually enough for practical use in simulation of pulse stamping methods. The point of FLD is obtained as a combination of thinning measured in the necking area and principal strains proportion obtained from numerical simulation using finite element code. The advantage of the developed method is the simplicity of used tooling, simplicity of measurement, no need to use meshes and expensive hardware and software to obtain strains. The experiment is conducted and the FLD is obtained for the stainless steel 12X18H10T (approximate US equivalent is S32100) of 0,55 mm.

REFERENCES

1. **Hallquist J.O.** LS-DYNA theoretical manual. Livermore Software Technology Corporation: Livermore, SA, 2006. 498 p.

2. **Dorel Banabic**. Sheet Metal Forming Processes. Constitutive Modelling and Numerical Simulation. Springer Heidelberg Dordrecht: London-New York, 2010. 301 p.

3. **Patent USSR № 697851** Ustroystvo dlia tarirovki p'ezoelektricheskih datchikov davleniia / Bogoiavlenskiy K.N., Vagin V.A., Mamutov V.S., Oreshenkov A.I. Prioritet 14.06.1979. (rus).

4. **Vagin V.A., Zdor G.N., Mamutov V.S.** Metody issledovaniya vysokoskorostnogo deformirovaniya metallov. Minsk: Nauka i tekhnika, 1990. 208 s. (rus).

5. **Aksenov L.B., Mamutov V.S., Mamutov A.V.** Postroenie diagramm predel'nyh deformaciy dlia prognozirovaniia razrusheniia tonkolistovoy zagotovki pri vysokoskorostnoy vytiazhke-formovke. *Forging-Stamping Production*. 2002. № 4. S. 9–12. (rus.)

6. **Persy J.N.** The effect of strain rate on the forming limit diagram for sheet metal. *Annals of CIPP*. 1980. Vol. 29. № 1. P. 131–132.

7. **Keeler S.P.** Rating the Formability of Sheet Metal. *Metal Progres*s. 1966. Vol. 90. P. 148–153.

8. **Goodwin G. M.** Application of Strain Analysis to Sheet Metal Forming Problems in the Press Shop. *Presented at SAE Automotive Engineering Congress*, Detroit (January 1968). Paper 680093, 8 p.

9. **Nakazima K., Kikuma T.** (1967) Forming limits under biaxial stretching of sheet metals. *Testu-to Hagane* 53:455–458 (in Japanese).

10. **Marciniak Z., Kuczynski K.** Limit strain in the process of stretch forming sheet metal. *International Journal of Mechanical Science*. Vol. 9. 1967. P. 609–620.

11. **Komarov A.D.** Shtampovka listovyh i trubchatyh detaley poliuretanom. Leningrad: LDNTP, 1975. 36 s. (rus).

12. **Mamutov A.V., Mamutov V.S.** Rascheti processov shtampovki podvizhnimi sredami pri pomoshi kompleksa LS-DYNA. *St. Petersburg State Polytechnical University Journal : Science and education*. 2012. № 2. Vol. 1 (147). S. 127–131. (rus).

СПИСОК ЛИТЕРАТУРЫ

1. **Hallquist J.O.** LS-DYNA theoretical manual. Livermore Software Technology Corporation: Livermore, CA, 2006. 498 p.

2. **Dorel Banabic**. Sheet Metal Forming Processes. Constitutive Modelling and Numerical Simulation. Springer Heidelberg Dordrecht: London-New York, 2010. 301 p.

3. **Патент СССР № 697851.** Устройство для тарировки пьезоэлектрических датчиков давления / Богоявленский К.Н., Вагин В.А., Мамутов В.С., Орешенков А.И. Приоритет 14.06.1979.

4. **Вагин В.А., Здор Г.Н., Мамутов В.С.** Методы исследования высокоскоростного деформирования металлов. Минск: Наука и техника, 1990. 208 с.

5. **Аксенов Л.Б. Мамутов В.С., Мамутов А.В.** Построение диаграмм предельных деформаций для прогнозирования разрушения тонколистовой заготовки при высокоскоростной вытяжке-формовке // КШП. 2002. № 4. С. 9–12.

6. **Persy J.N.** The effect of strain rate on the forming limit diagram for sheet metal // Annals of CIPP. 1980. Vol. 29. № 1. P. 131–132.

7. **Keeler S.P.** Rating the Formability of Sheet Metal // Metal Progress. 1966. Vol. 90. P. 148–153.

8. **Goodwin G.M.** Application of Strain Analysis to Sheet Metal Forming Problems in the Press Shop //Presented at SAE Automotive Engineering Congress. Detroit. January 1968. Paper 680093, 8 p.

9. **Nakazima K., Kikuma T.** (1967) Forming limits under biaxial stretching of sheet metals // Testu-to Hagane 53:455–458 (in Japanese).

10. **Marciniak Z., Kuczynski K.** Limit strain in the process of stretch forming sheet metal // International Journal of Mechanical Science. 1967. Vol. 9. P. 609–620.

11. **Комаров А.Д.** Штамповка листовых и трубчатых деталей полиуретаном. Л.: ЛДНТП, 1975. 36 с.

12. **Мамутов А.В., Мамутов В.С.** Расчеты процессов штамповки подвижными средами при помощи комплекса LS-DYNA // Научно-технические ведомости СПбГПУ. Наука и образование. 2012, № 2. Vol. 1 (147). С. 127–131.

СВЕДЕНИЯ ОБ АВТОРАХ/AUTHORS

MAMUTOV Viatcheslav S. – Peter the Great St. Petersburg Polytechnic University.
29 Politechnicheskaya St., St. Petersburg, 195251, Russia.
E-mail: mamutov_vs@spbstu.ru

МАМУТОВ Вячеслав Сабайдинович – доктор техн. наук профессор Санкт-Петербургского политехнического университета Петра Великого.
195251, Россия, г. Санкт-Петербург, Политехническая ул., 29.
E-mail: mamutov_vs@spbstu.ru

MAMUTOV Aleksandr V. – Oakland University.
2200 N Squirrel Rd. Rochester, Michigan, 48309.
E-mail: a.mamutov@yahoo.com

МАМУТОВ Александр Вячеславович – кандидат технических наук приглашенный ученый Окландского университета
48309, США, Мичиган, 2200 N Squirrel Rd. Rochester.
E-mail: a.mamutov@yahoo.com

KUNKIN Sergei N. – Peter the Great St. Petersburg Polytechnic University.
29 Politechnicheskaya St., St. Petersburg, 195251, Russia.
E-mail: ksn54@mail.ru

КУНКИН Сергей Николаевич – кандидат технических наук доцент Санкт-Петербургского политехнического университета Петра Великого.
195251, Россия, г. Санкт-Петербург, Политехническая ул., 29.
E-mail: ksn54@mail.ru

ARSENTYEVA Kseniia S. – Peter the Great St. Petersburg Polytechnic University.
29 Politechnicheskaya St., St. Petersburg, 195251, Russia.
E-mail: fartran@li.ru

АРСЕНТЬЕВА Ксения Сергеевна – аспирант Санкт-Петербургского политехнического университета Петра Великого.
195251, Россия, г. Санкт-Петербург, Политехническая ул., 29.
E-mail: fartran@li.ru